Linearity Error Report for the
LWP, LWR and SWP cameras

Nancy A. Oliversen

I. Introduction

Standard star spectra, obtained between March 1983 and March 1984, have been analyzed to monitor the linearity errors of non-optimum exposures. The observation and analysis techniques used in this report are briefly summarized in section II. The reproducibility of optimum trailed spectra for all three cameras is discussed in section III. Linearity errors for non-optimum spectra are discussed in section IV. Finally, linearity errors for spectra with high backgrounds is discussed in section V.

II. Observation and Data Analysis Technique

The observation and analysis technique used for this study is similar to the method used in Oliversen (1983). The standard star HD 60753 is used for most of this linearity report. Linearity monitoring spectra are normally obtained twice a year, in March and in September. The linearity errors are determined by ratioing a test image with a standard 100% exposure level image with low background. The spectral ratios are then smoothed with a 5 point median filter and with an 11 point boxcar filter.

To minimize the effects of long term sensitivity variations (Sonneborn and Garhart, 1983), one should compare spectra obtained on the same day. This was not always possible for the high background spectra due to scheduling constraints. In these cases the reference spectra were obtained within a month of the test spectra. A change in the camera head amplifier temperature (THDA) during the exposure sequence also causes the camera sensitivity to change (Sonneborn and Garhart, 1983). All ratios have been corrected for this temperature-induced sensitivity change.

III. Reproducibility

Figures 1 and 2 show the ratio of fluxes from pairs of identical, optimally-exposed trailed spectra of HD 60753. The flux ratios were averaged over 100 angstrom bandpasses and are listed in Table 1. Including the data from the previous report, five pairs of optimum trailed SWP and LWR spectra obtained between 1981 and September 1983 have been analyzed. The reproducibility of the SWP and LWR cameras appears to be slightly better than the values reported in Oliversen (1983). The binned flux ratios for the SWP camera show an rms deviation of 2.5% from unity and the LWR flux ratios 1.2% from unity. The reproducibility of the LWP camera appears to be slightly poorer than the LWR, with an rms deviation from unity of 2.2%. It should be noted that the above LWP value is based on only two pairs of 100% spectra obtained in March and September 1983. As additional LWP linearity monitoring data are obtained this value may be modified somewhat. The rms and average reproducibility for the three cameras is also listed in Table 1.

IV. Linearity Errors for Non-optimum Spectra

Figures 3 through 8 illustrate typical linearity errors for a variety of non-optimum exposure levels. Sample 40%/100% and 120%/100% flux ratios averaged over 100 angstrom bandpasses are also listed in Table 2.

Figures 3 through 6 show the flux ratios of 30%/100% (March and September 1983), 40%/100% (March 1983), 40%/100% (September 1983), and 60%/100% (March, 1983), respectively. The flux ratios for the SWP and LWR cameras show the same general pattern of linearity errors as described in Oliversen (1983). For the LWR, as the exposure level is reduced, the derived flux is too high relative to the flux for an optimum exposure level. For the SWP, the flux ratio is a function of wavelength. At the shortest wavelengths, the derived flux is too low relative to an optimum exposure, while at the longest wavelengths the flux is too high.

Figure 4a shows the flux ratio for a 40%/100% LWP pair. The flux ratio is curved as a function of wavelength and is very noisy. The derived flux between about 2400 and 3000 A is too low relative to the optimum exposure by 4 to 6%. At the ends of the spectrum, the flux ratio appears to curve upward slightly towards unity.

V. Linearity Errors for Spectra with High Backgrounds

Figures 9 and 10 illustrate linearity errors for spectra obtained with high backgrounds. The flux ratios averaged over 100 angstrom bandpasses are listed in Table 3. The average peak background levels for the test spectra were between 95 to 110 DN. The average peak continuum levels were between 180 and 200 DN.

The images in figure 9 were produced by exposing the camera to an non-optimum (40%) trailed stellar image and then superimposing a tungsten flood lamp exposure. For the SWP camera the high tungsten flood background flux ratio is a function of wavelength. At the shortest wavelengths the derived flux is too high by about 3% relative an the optimum exposure, while at the longest wavelengths the derived flux is too low by about 7%. This slope is reversed from the slope seen in the low background 40%/100% ratios.

For the LWR camera the derived flux ratio for a high background, underexposed image is also a function of wavelength. At the shortest wavelengths the derived flux ratio was about 25% lower than the derived flux for an optimum exposure, while at the longest wavelengths the flux ratio was about 8% low.

The average of the high t-flood background LWP ratio is near unity. The ratio also displays large fluctuations between sections which are 100 to 200 Angstroms in size.

Previous high background studies have used the tungsten flood as a way of mimicking the background induced by the field particle radiation. This has been done primarily because the spectra can be obtained at any time. However, the pattern of background across the camera faceplate is known to be different for the tungsten flood and radiation backgrounds, which may result in a different pattern of linearity errors for the two. Consequently, the test images for figure 10 were produced by exposing the camera to a non-optimum (40%) trailed stellar image and then exposing the camera to empty sky to build up the radiation-induced background level.

Comparison of Figures 9 and 10 shows that the linearity errors for underexposed spectra with high tungsten-flood versus high radiation backgrounds do differ in some aspects. The flux ratio for the radiation background SWP exposures are flatter compared to the tungsten flood background exposures. The derived flux for the radiation background exposure was too high by 2 to 6% compared to the optimum exposure.

The linearity errors for the radiation background LWR exposure appear to be smaller compared to the t-flood background exposures. The derived flux between 2500 and 2800 angstroms for the radiation background exposure was too high by 4 to 8%.

The flux ratio for the radiation background LWP exposures are similar to the tungsten flood background exposures. They both display a similar pattern of alternating sections of high and low flux ratios. For both, in the 2200 to 2300 angstrom region, linearity errors are particularily poor, with derived fluxes too high by about 19%.

VI. Summary

The reproducibility of trailed SWP (2.2%) and LWP (2.5%) spectra is slighlty poorer than LWR (1.2%) spectra. All three cameras show significant linearity errors for under exposed spectra. The general characteristics of the linearity errors appear to be similar to earlier linearity monitoring data, however further quantitative analysis is needed to determine if there have been any small scale changes in the linearity. Under-exposed trailed spectra with high tungsten flood or radiation-induced backgrounds also have large linearity errors. Errors of up to 10 to 20% are not uncommon. The characteristics of the radiation-induced background errors differ from the tungsten flood backgrounds. On the average, the radiation-induced background non-linearities seem to be less severe than the tungsten flood background non-linearities.

References

Oliversen, N. A. 1983, NASA IUE Newsletter, No. 23, p. 31.

Sonneborn, G. and Garhart, M. P. 1983, NASA IUE Newsletter, No. 23, p. 23.

Table 1

Binned Reproducibility Errors

Central Wavelength	Flux Ratios March 1983 (fig 1) SWP	LWR	LWP	September 1983 (fig 2) SWP	LWR	LWP
1300	0.972			0.998		
1400	0.979			0.995		
1500	0.991			1.004		
1600	0.978			1.003		
1700	0.987			0.998		
1800	0.991			0.999		
1900	0.989			1.005		
2100		0.997	0.987		1.006	1.003
2200		0.998	0.985		1.011	1.013
2300		1.007	0.950		1.006	1.005
2400		1.003	0.986		1.007	0.998
2500		1.014	0.974		1.003	0.991
2600		1.008	0.960		0.998	0.981
2700		1.000	0.976		0.999	0.982
2800		1.004	0.970		1.000	0.999
2900		0.992	0.978		1.000	0.987
3000		1.002	0.989		1.008	0.981

	SWP[a]	LWR[a]	LWP[b]
RMS Dev.	2.52%	1.17%	2.17%
Ave Dev.	1.91%	0.90%	1.74%

[a] Five pairs of 100% spectra used (late 1981, Mar. 1982, Sept. 1982, Mar. 1983 and Sept. 1983).

[b] Two pairs of 100% spectra used (Mar. 1983 and Sept. 1983).

Also Note:

Ave Dev = ave[abs(1-FR)]

RMS Dev = $[\sum (FR-1)^2]^{1/2} / (n-1)$

Table 2

Binned Flux Ratios for Non-Optimum Exposure Levels
March 1983 (Figures 4 and 7)

Central Wavelength	Flux Ratios 40%/100% SWP	LWR	LWP	120%/100% SWP	LWR	LWP
1300	0.958			1.005		
1400	0.974			1.005		
1500	0.996			1.002		
1600	0.992			0.995		
1700	1.009			1.002		
1800	1.020			0.999		
1900	1.036			0.999		
2100		1.027	1.024		0.998	0.973
2200		1.012	1.004		1.009	1.002
2300		1.052	1.043		0.995	0.988
2400		1.074	0.977		1.013	1.001
2500		1.104	0.978		1.004	0.987
2600		1.093	0.952		0.999	0.977
2700		1.067	0.960		1.005	0.977
2800		1.073	0.953		1.015	0.988
2900		1.054	0.952		1.022	0.994
3000		1.077	0.973		0.998	1.005
3100		0.995	0.997		0.996	1.014

Table 3

Binned Flux Ratios for High Background Spectra

Central Wavelength	40%/100% Flux Ratios: Tflood Bkgs. (Fig. 9a,b) SWP	LWR	LWP	Radiation Bkgs. (Fig. 10a,b) SWP	LWR	LWP
1300	1.033			1.019		
1400	1.024			1.038		
1500	1.021			1.035		
1600	0.959			1.064		
1700	0.985			1.016		
1800	0.963			1.022		
1900	0.935			1.040		
2100		0.753	1.073		0.971	0.995
2200		0.835	1.079		0.927	1.193
2300		0.911	1.001		0.968	1.083
2400		0.860	1.018		1.016	1.006
2500		0.904	1.017		1.086	1.053
2600		0.938	1.046		1.041	1.043
2700		0.937	0.991		1.047	1.031
2800		0.906	0.975		1.065	1.012
2900		0.940	1.036		1.027	1.036
3000		0.917	1.066		0.993	1.084

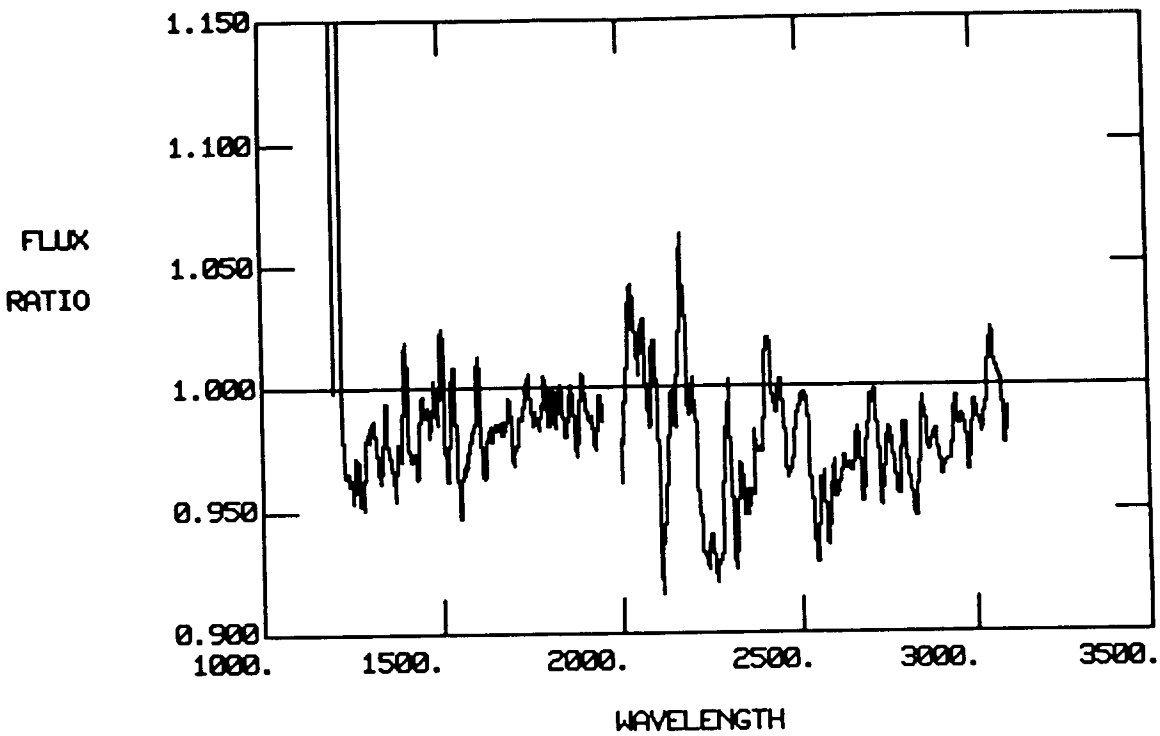

Figure 1a. Reproducibility 100%/100%
SWP 19409 / SWP 19414
LWP 1821 / LWP 1826
March, 1983

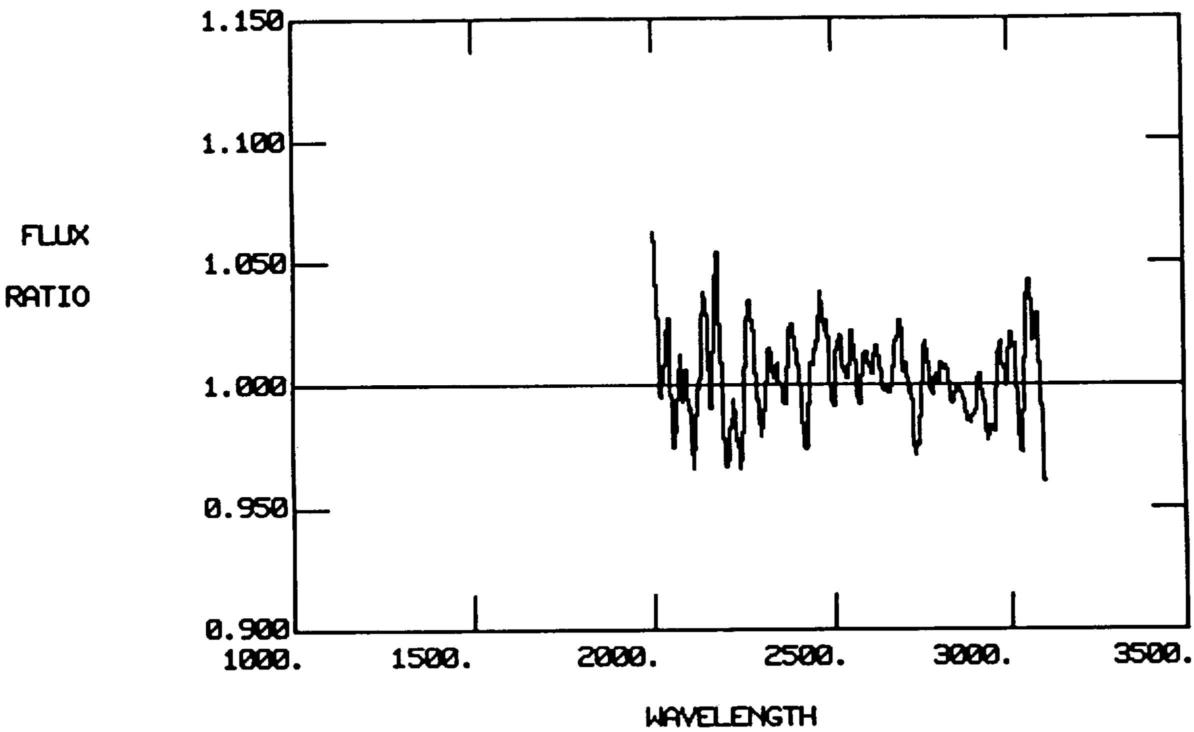

Figure 1b. Reproducibility 100%/100%
LWR 15553 / LWR 15557
March, 1983

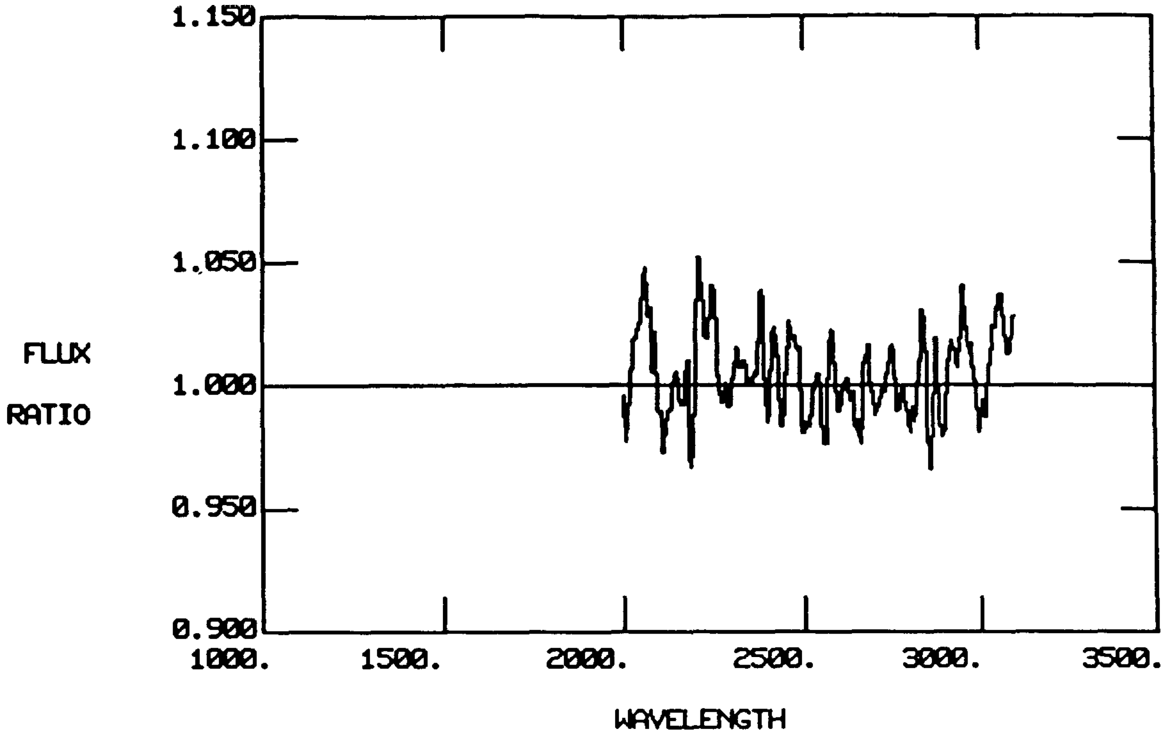

Figure 2b. Reproducibility – 100% / 100%
LWR 16785 / LWR 16789
September, 1983

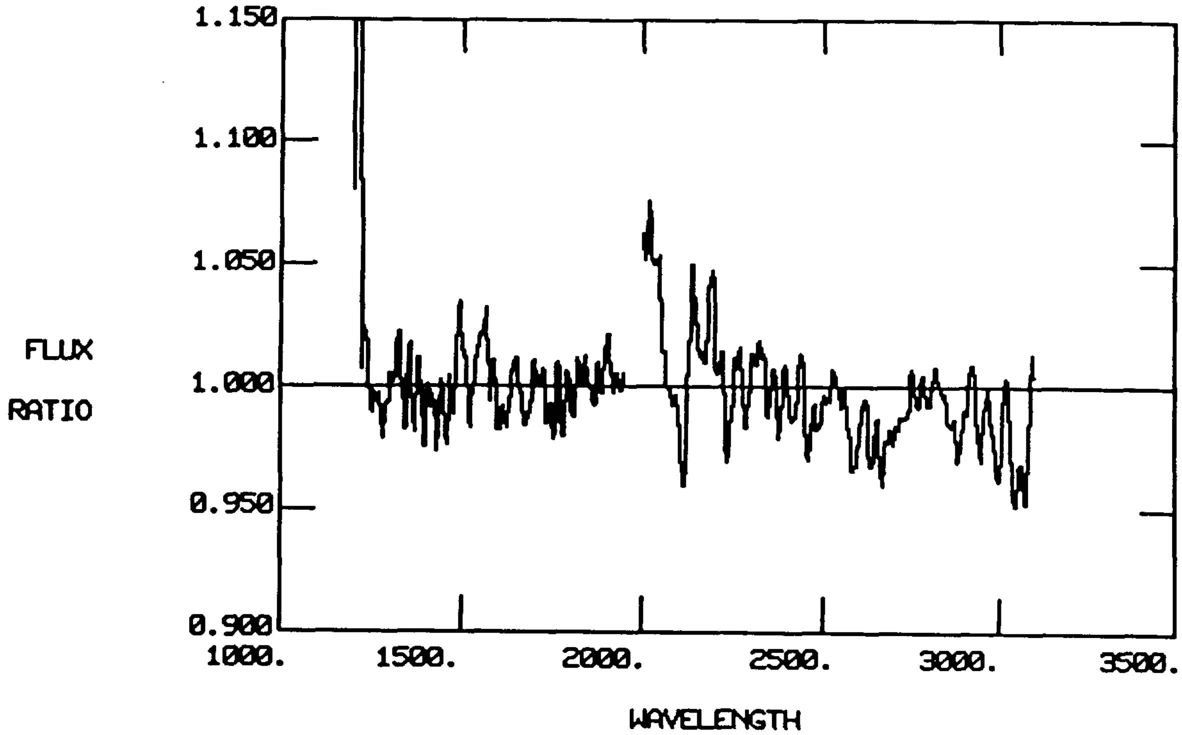

Figure 2a. Reproducibility – 100%/100%
SWP 21041 / SWP 21045
LWP 1997 / LWP 2000
September, 1983

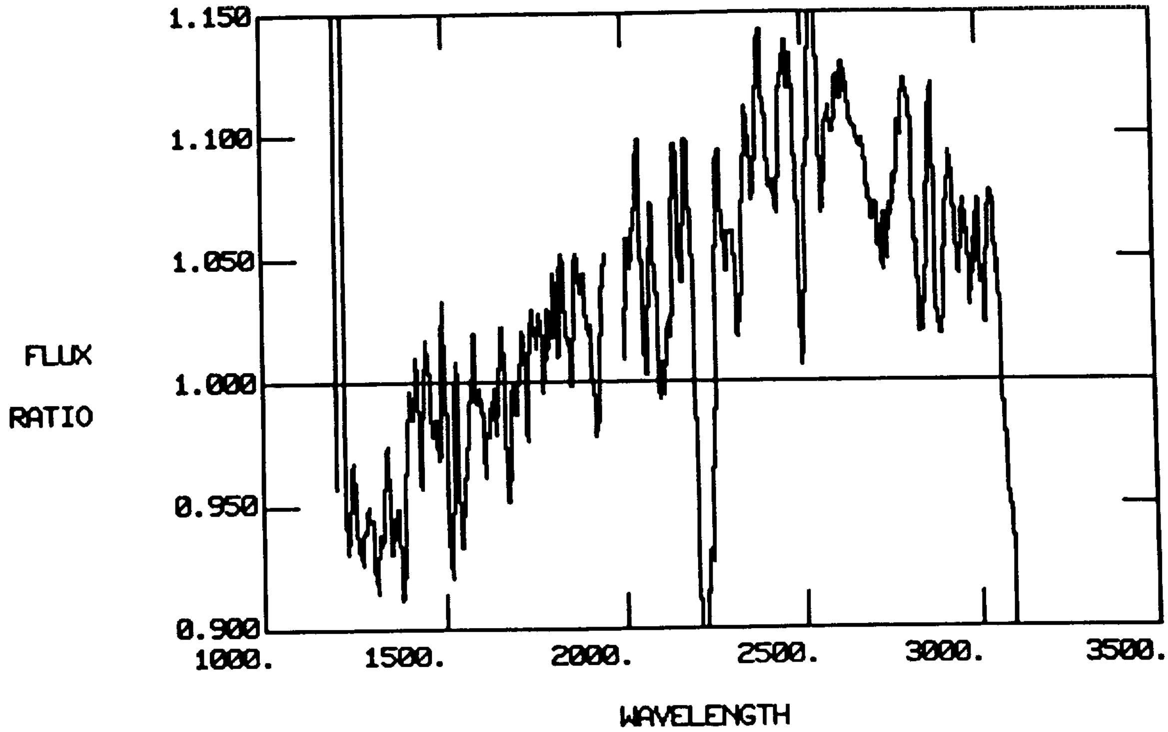

Figure 3a. 30% / 100% for March, 1983
SWP 19410 / SWP 19414
LWR 15554 / LWR 15557

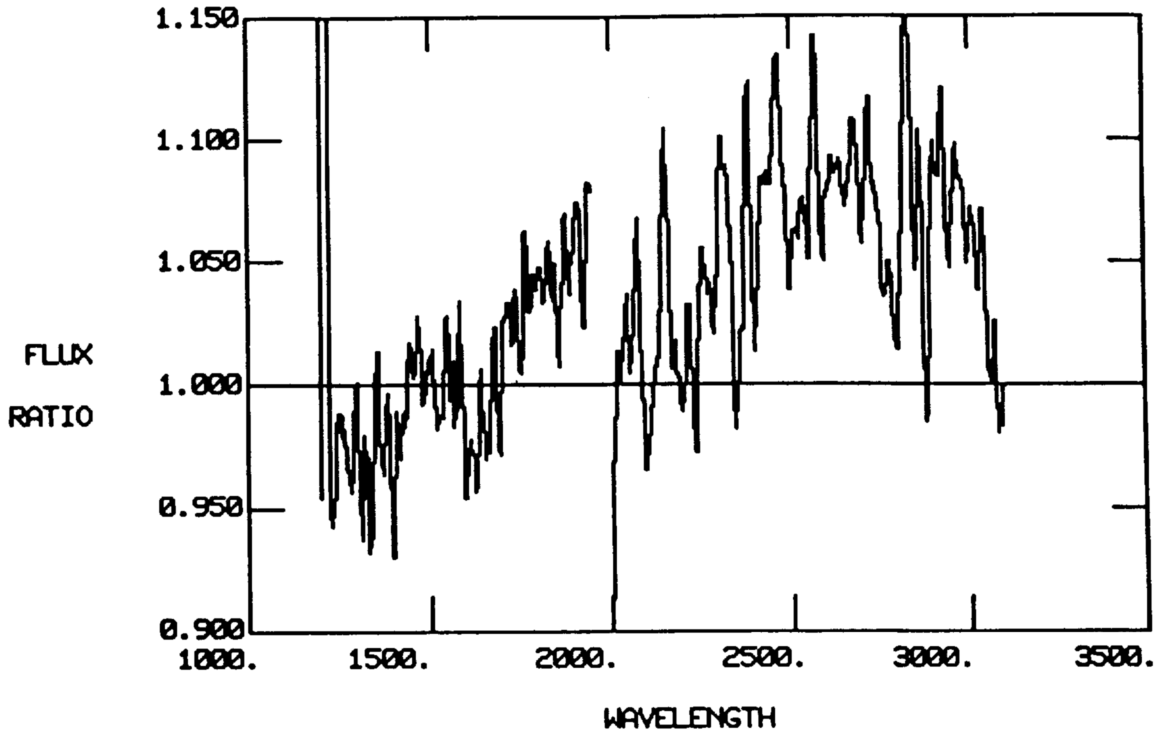

Figure 3b. 30% / 100% for September, 1983
SWP 21042 / SWP 21045
LWR 16786 / LWR 16789

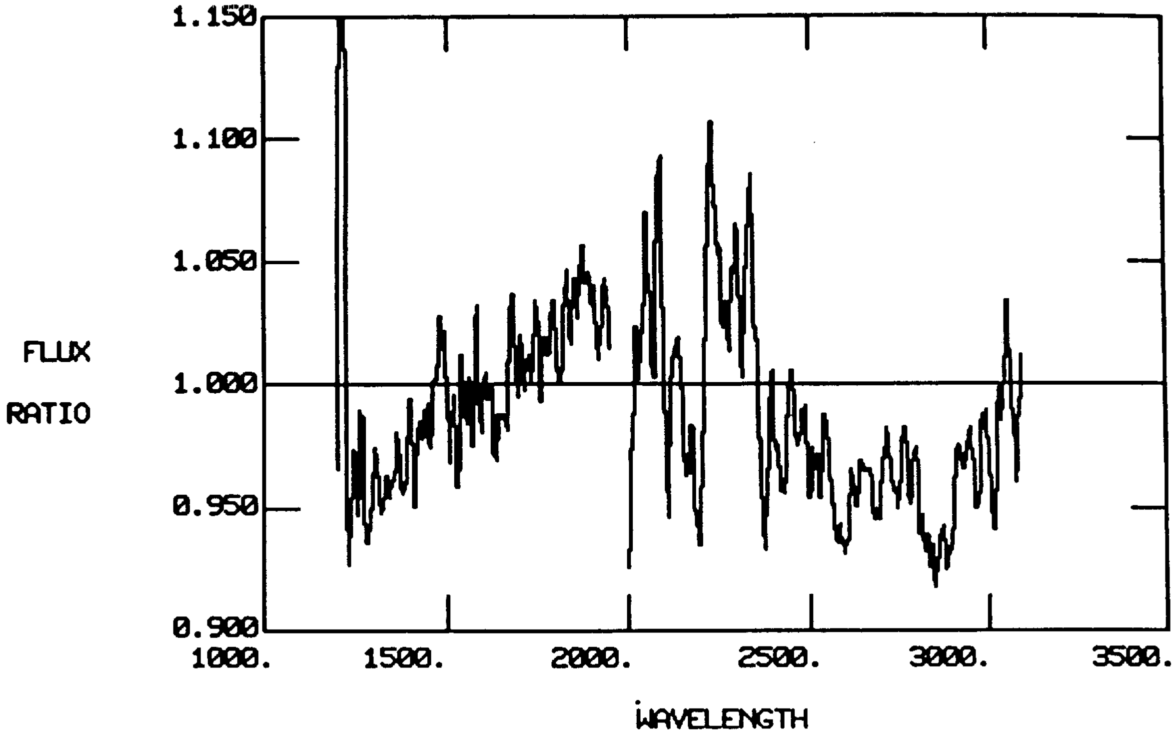

Figure 4a. 40% / 100% for March, 1983
SWP 19412 / SWP 19414
LWP 1824 / LWP 1826

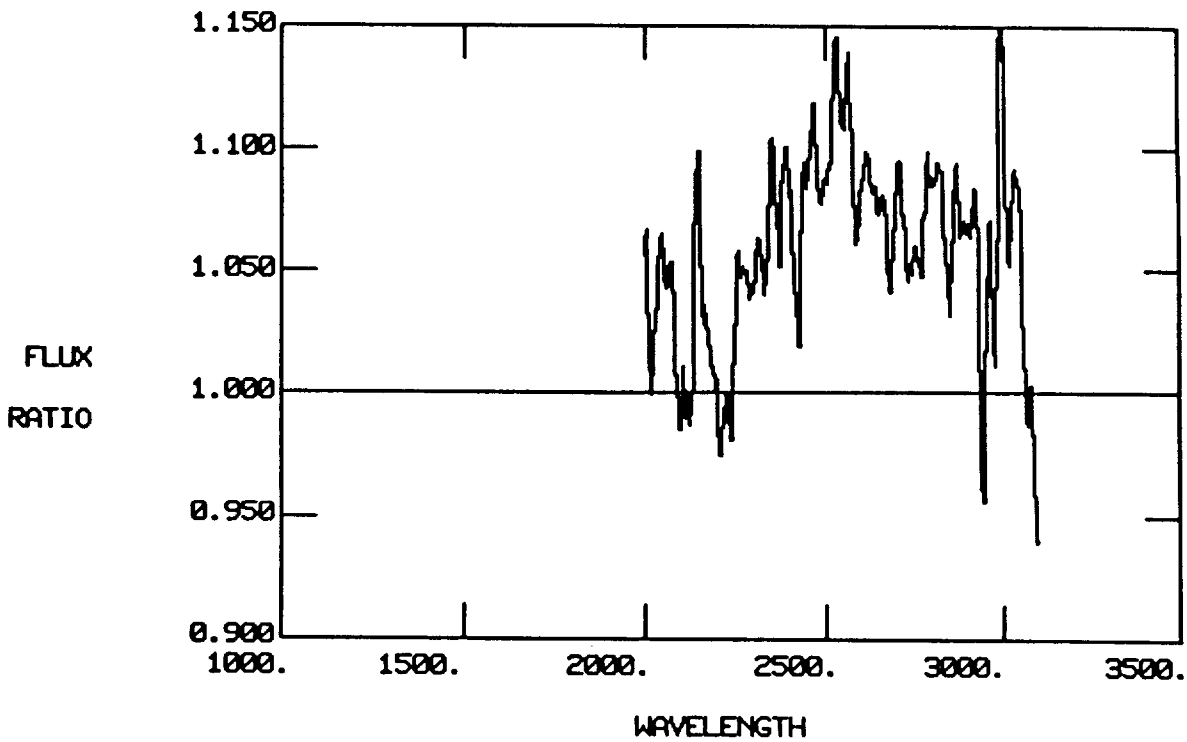

Figure 4b. 40% / 100% for March, 1983
LWR 15556 / LWR 15557

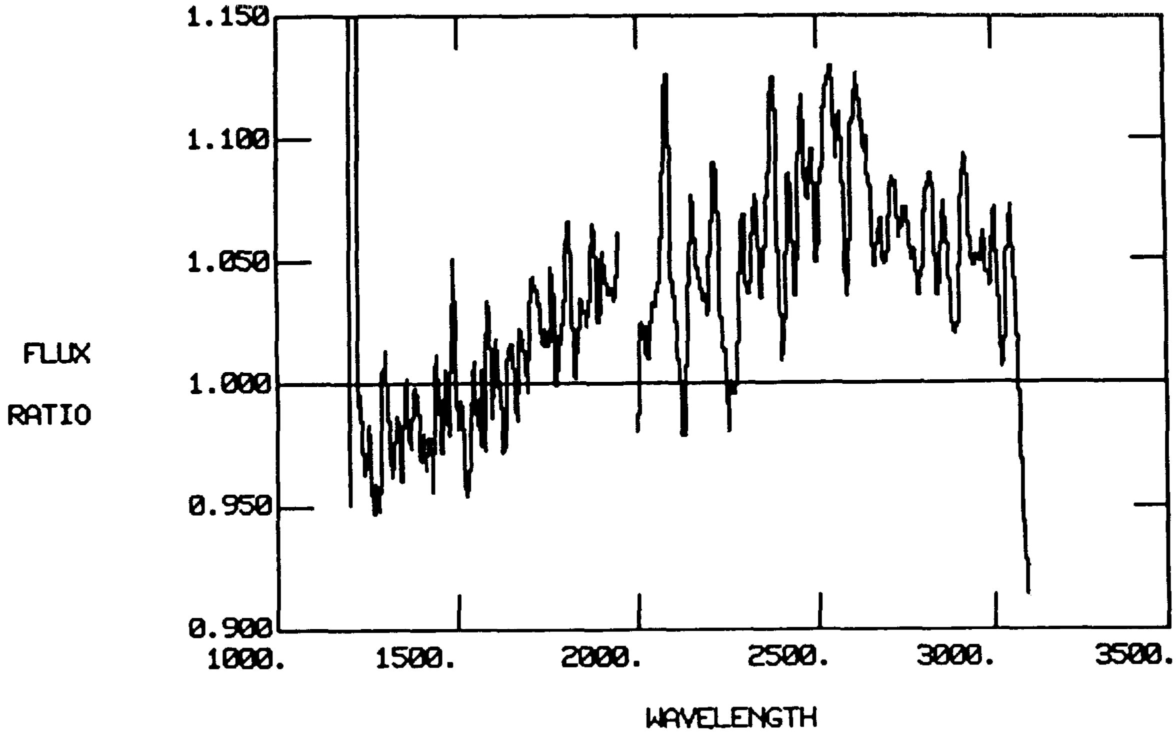

Figure 5 . 40% / 100% for September, 1983
SWP 21044 / SWP 21045
LWR 16788 / LWR 16789

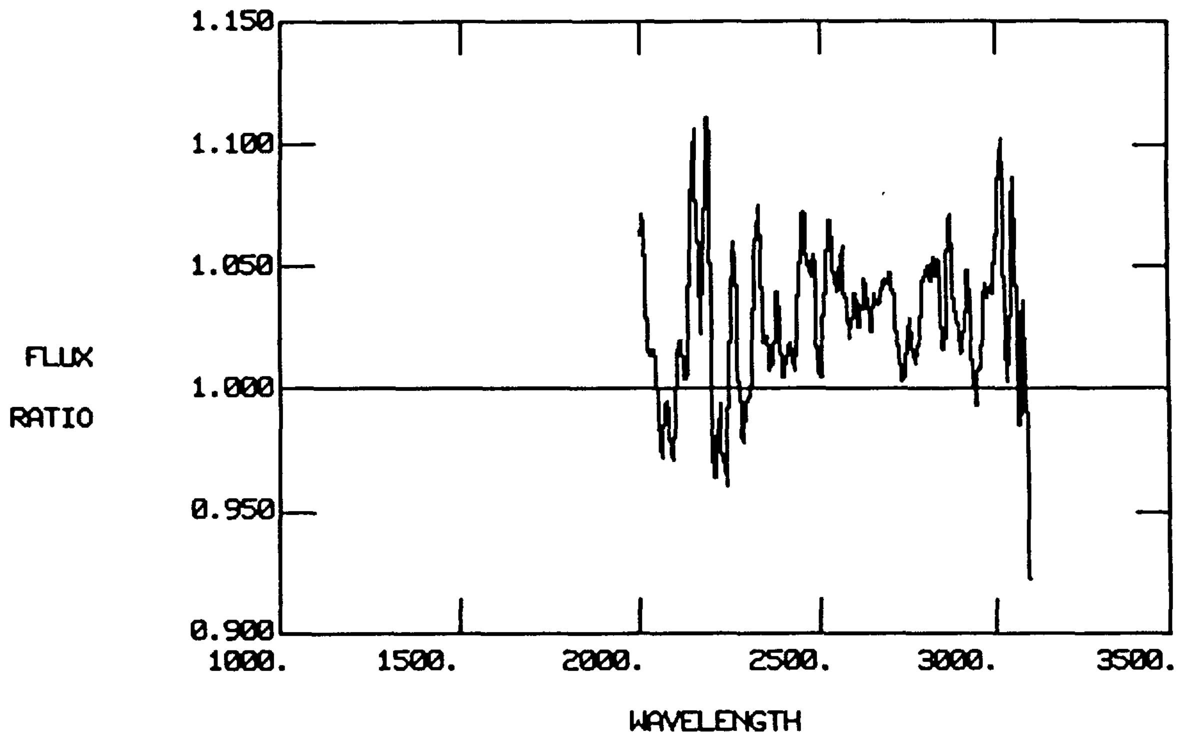

Figure 6 . 60% / 100% for March, 1983
LWR 15559 / LWR 15557

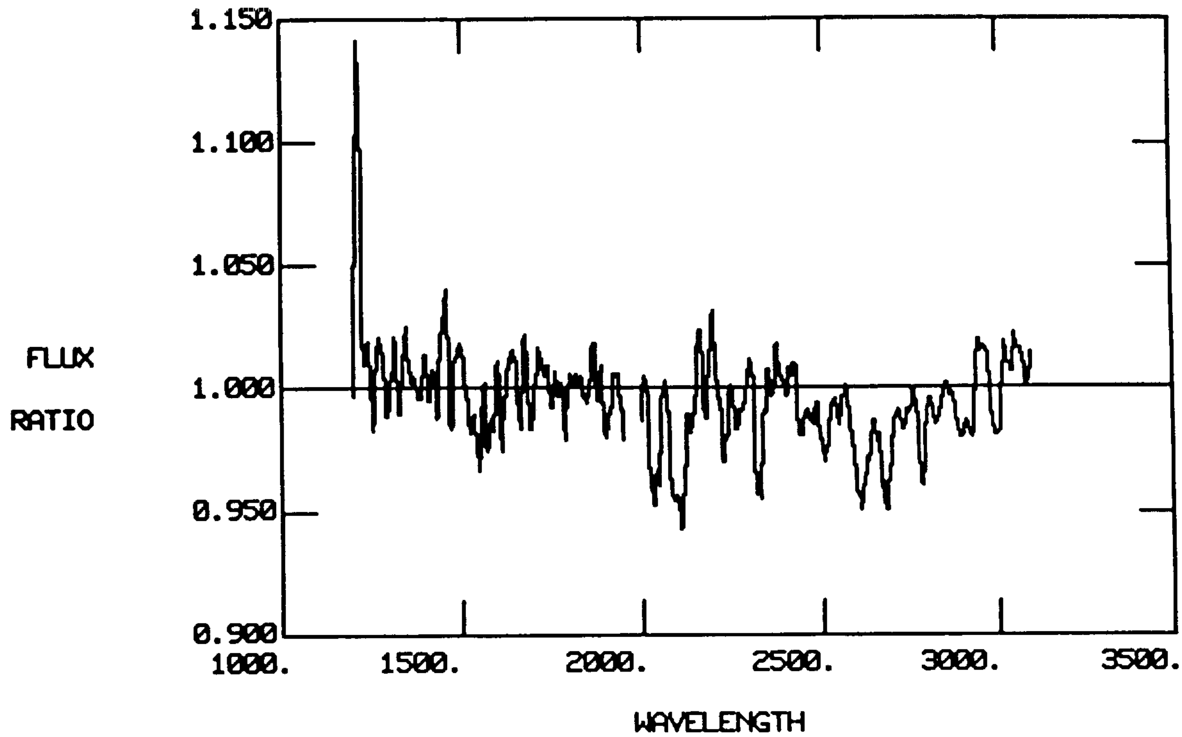

Figure 7a. 120% / 100% for March, 1983
SWP 19411 / SWP 19414
LWP 1823 / LWP 1826

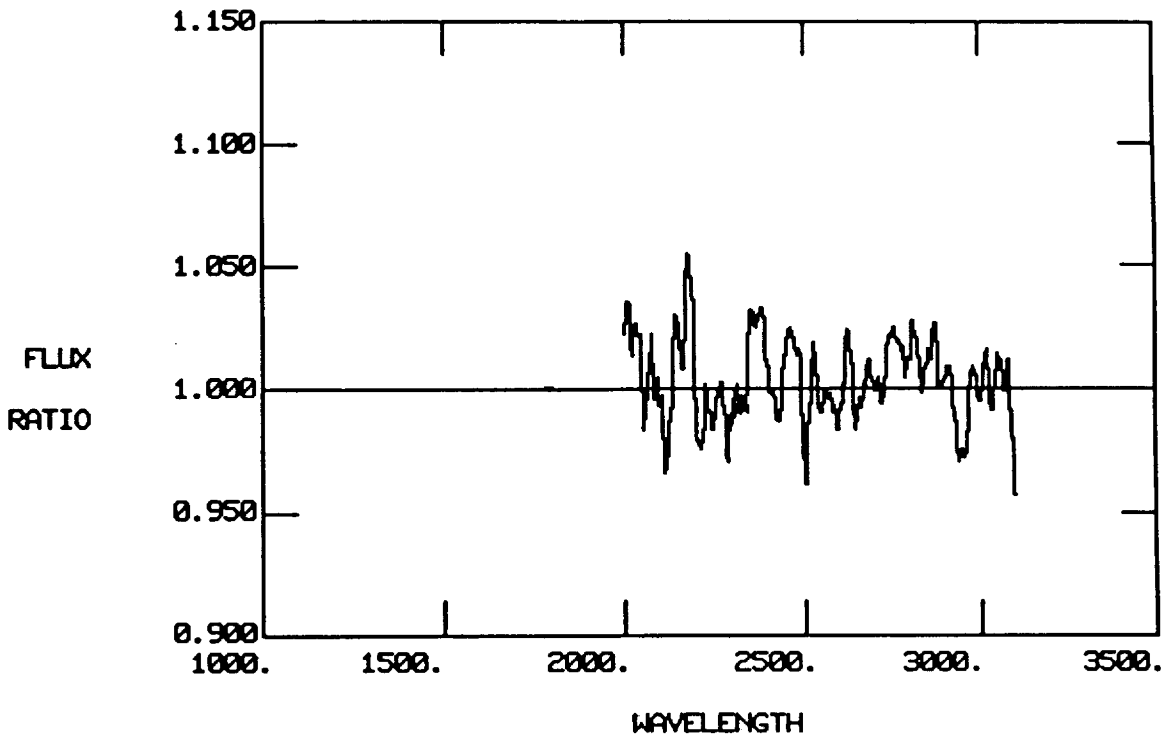

Figure 7b. 120% / 100% for March, 1983
LWR 15555 / LWR 15557

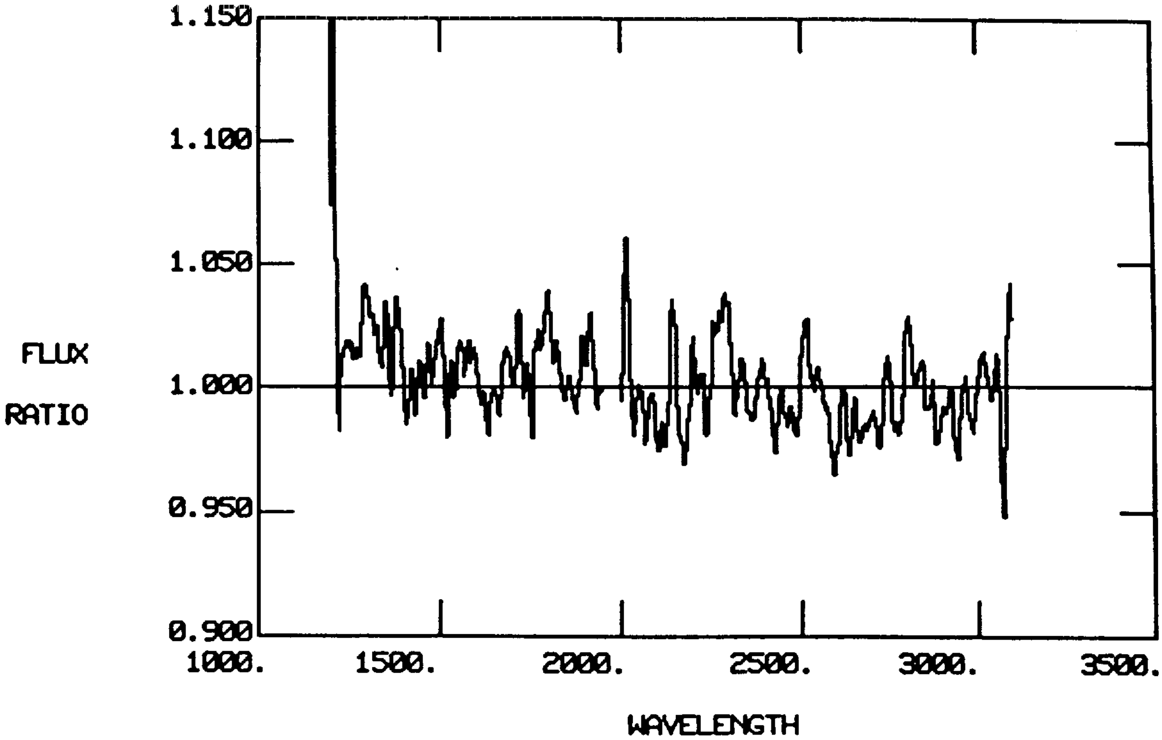

Figure 8a. 120% / 100% for September, 1983
SWP 21043 / SWP 21045
LWP 1999 / LWP 2000

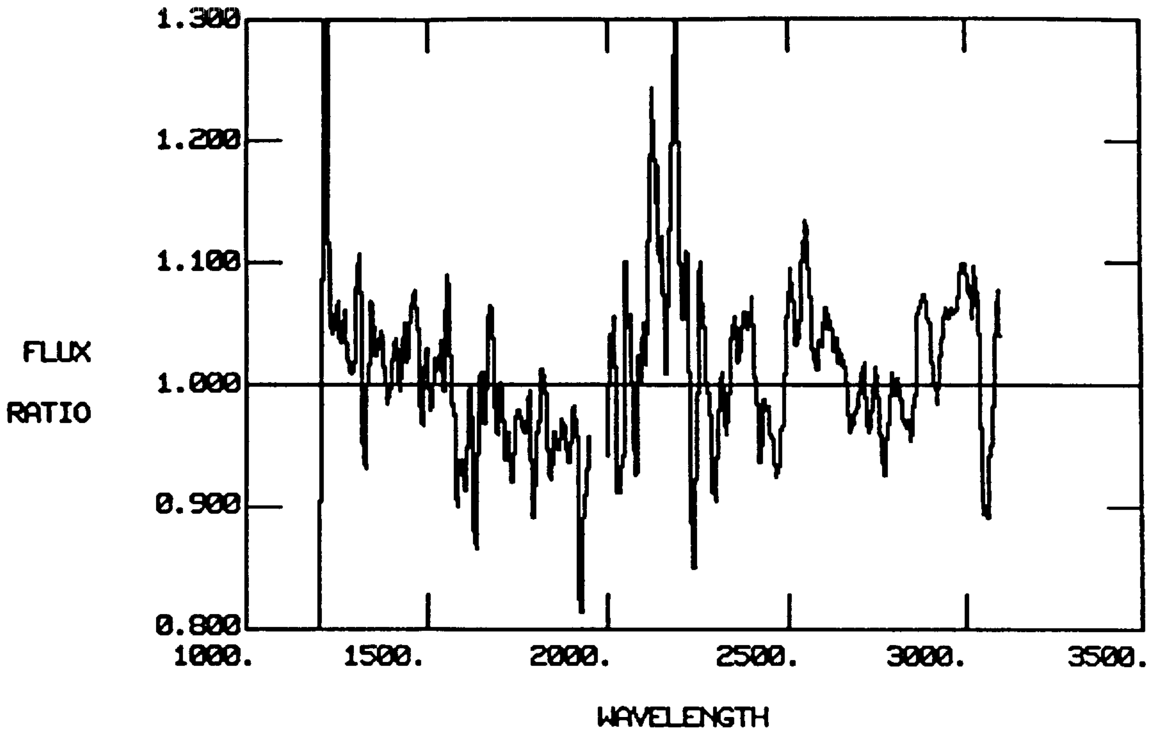

Figure 9a. (40% + high TFLOOD bdg) / 100%
February, 1984
SWP 22267 / SWP 22269
LWP 2769 / LWP 2770

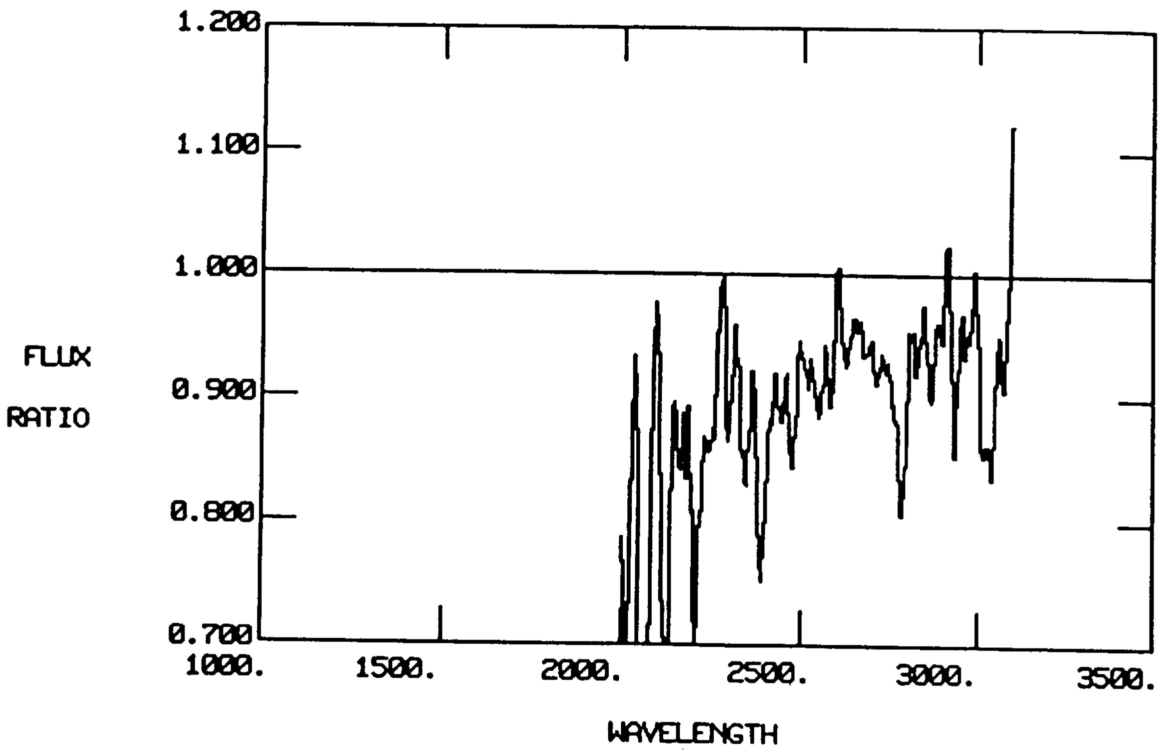

Figure 9b. (40% + high TFLOOD bkg) / 100%
HD 60753 February, 1984
LWR 17249 / LWR 17250

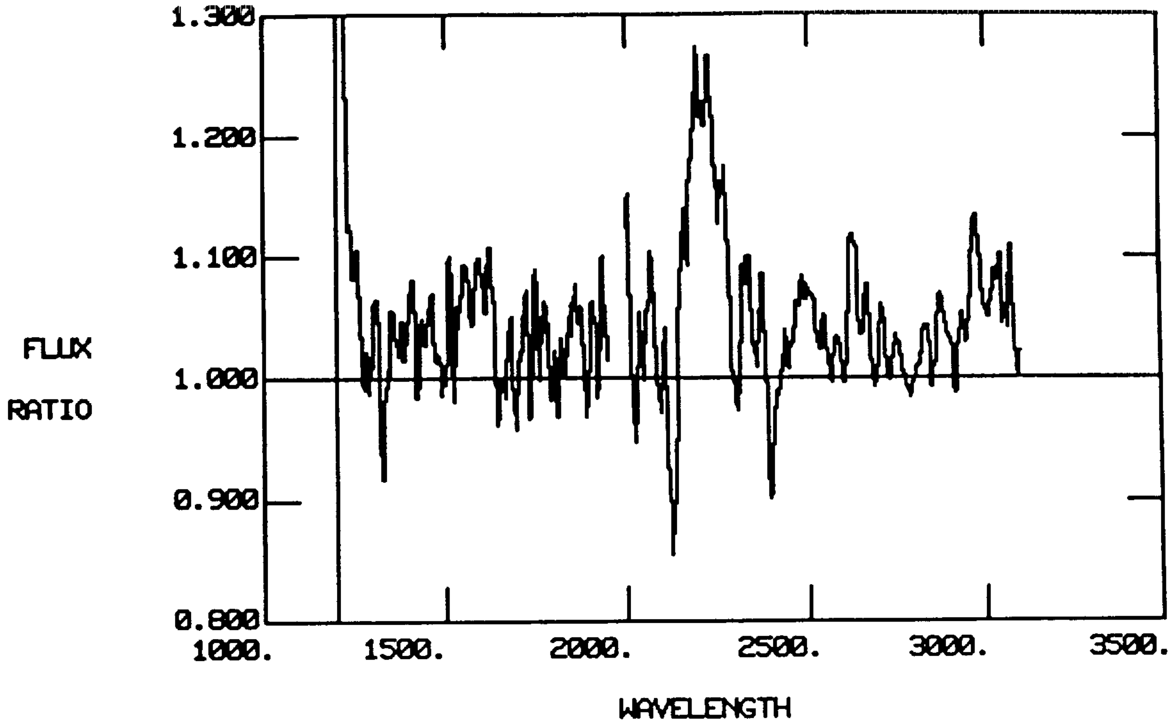

Figure 10a. (40% + high radiation bkg) / 100%
HD 60753 March, 1984
SWP 22420 / SWP 22572
LWP 2896 / LWP 2951

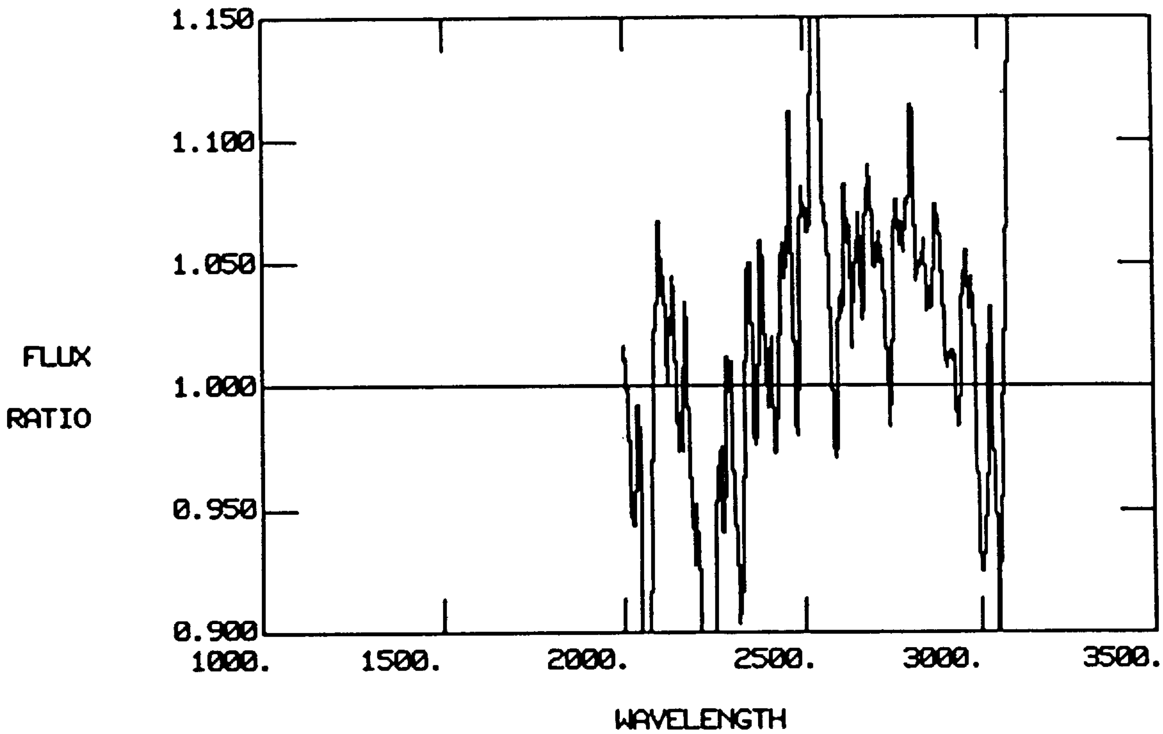

Figure 10b. (40% + high radiation bkg) / 100%
HD 60753 March, 1984
LWR 17280 / LWR 17319